Roton-like dispersion via polarisation change for elastic wave energy control in graded delay-lines

L. Iorio [*], J.M. De Ponti, F. Maspero, R. Ardito

Department of Civil and Environmental Engineering, Politecnico di Milano, Piazza Leonardo da Vinci, 32, 20133 Milano, Italy

A R T I C L E   I N F O

A B S T R A C T

While roton dispersion relations had been restricted to correlated quantum systems at low temperature, recent works show the possibility of obtaining this unusual dispersion in acoustic and elastic metamaterials. Such phenomenon has been demonstrated in periodic structures by means of beyond-nearest-neighbour interactions, following the formulation firstly developed by Brillouin in the '50s. In this paper, we demonstrate both numerically and experimentally that beyond-nearest-neighbour connections are not a necessary condition to obtain this unusual dispersion relation in elasticity. Leveraging the intrinsic complexity of elastic systems supporting different types of waves, we demonstrate that mode locking can be applied to obtain roton dispersion, without the need of elastic or magnetic interactions between non nearest neighbours. Moreover, the combination of roton dispersion and rainbow physics enables spatial separation of the energy fluxes with positive and negative group velocity.

1. Introduction

Elastic and acoustic wave manipulation through the use of metamaterials and phononic crystals has been received increasing attention in the last two decades thanks to the exotic and non common dynamic properties of such structures.

While early designs were based on Bragg scattering or local resonance to create wide and low-frequency band-gaps [1–7], consideration is now transitioning to more complete forms of wave control, including energy focusing and amplification [8–10], wave filtering [11] and conversion [12], beam-splitting [13], robust signal communication [14] and localisation [15] using concepts from topological insulators [16–18]. The possibility to control wave energy is always related to the design of properly engineered dispersion relations, with the concurrent creation of band-gaps and peculiar eigenstates. In topologically based metamaterials, protected edge (or interfacial) surface states are achieved by leveraging broken symmetries in time [19–21] or space [22,22,23], emulating the Quantum Hall (QHE) or Quantum Spin Hall (QSHE) effects. In graded-based systems, band-gaps are spatially controlled to emulate lensing or rainbow effects for signal amplification [9,24] or energy conversion [25,26]. Broadly speaking, a large number of studies have been devoted to shaping the wave dispersion curves, creating phononic, locally resonant or topological band-gaps, often combined together to obtain unusual behaviours.

Very recently, theoretical [27] and experimental studies [28] in acoustics and elasticity show the possibility of tailoring the lowest dispersion branch to achieve a so-called *roton-like* dispersion. Generally the term, most certainly for elastic waves, has been used to describe dispersion relations of a material that shows two points of zero-group velocity (one is a relative maximum and the other a relative minimum). The term originated in quantum physics from the peculiar dispersion of the quasi-particle Helium-4, that shows a decrease in momentum when the energy of the particle is increased [29,30]. This is due to the generation of a

---

* Corresponding author.
  E-mail address: luca.iorio@polimi.it (L. Iorio).

relative rotation of the particles that effectively reduces the momentum of each particle in a specific energy region [31,32]. The term has been then expanded to the realm of designed crystals or periodic metamaterials, even though the involved phenomena are physically very different. Such unusual dispersion has been obtained using chiral crystals with hybridisation of the microrotational and translational modes [33] or by means of non nearest-neighbour interactions. The idea of using Lth neighbour interactions to get multiple wavelengths at a given frequency, i.e. dispersion curves with multiple maxima and minima, was firstly developed by Brillouin [34] in the $'50s$, with a complete discussion about the distance of interaction in lumped systems. Such ideas have been recently revitalised, designing engineered structures with non-nearest-neighbour interactions by means of elastic connections [27,28] or thanks to electrostatic or magnetic forces [35–37]. While both approaches enable the effective design of a so-called roton-like dispersion curve, they imply complex manufacturing techniques. Specifically, non-nearest-neighbour interactions based on elastic connections require three dimensional setting to avoid overlap in two dimensions [27,28]. This can be a serious limitation for many applications, e.g. in Micro-electromechanical systems (MEMS) [38] or large structures which cannot rely on 3D-printing technologies. On the other hand, the mathematical model of the second approach is more difficult, given the intrinsic non-linear nature of the magnetic or electrostatic interaction, and manufacturing issues can arise in creating complex elasto-magnetic structures.

On this paper, we propose alternative and simpler structures, which can be easily manufactured in two-dimensional settings without the need of complex arrangements of elastic connections or non-linear magnetic forces.

The method we propose is general for elastic systems, and allows to obtain the same dispersion relation characteristics as the works described above, but not relying on coupling between cells far apart. The underlying physics is based on the peculiar properties of elastic systems, i.e. their capability to naturally support different types of waves, each one with a specific wavelength, polarisation and velocity. Since an elastic medium simultaneously support different propagating modes with different wave speeds, a coupling between them automatically activates non-nearest-neighbours without the necessity of extra elastic links or forces.

This approach relies on a physical phenomenon known in physics as mode locking [39], and recently proposed to achieve rainbow trapping [40] and selective mode conversion [41,42] in elastic waveguides. By breaking symmetries along the wave propagation direction, a strong coupling between different modes is achieved granting, at a given frequency, waves with equal and opposite group velocity. Specifically, we design an arrangement of resonators able to couple three different types of wave: torsional (T), flexural in-plane (F_{ip}) and flexural out-of-plane (F_{op}), each one with a specific wavelength λ, polarisation p, phase v_{ph} and group v_g velocity.

The concept of coupling and the consequent roton-like dispersion is schematically reported in Fig. 1, where the periodic structure that couples the three modes is shown. The modes are also schematically depicted in Fig. 1(a) (red: torsional, violet: in-plane flexural, green: out-of-plane flexural), while Fig. 1(b) shows the dispersion relation of the elementary cell colour coated with respect to the mode described. The coupling between T, F_{op} and F_{ip} is achieved by placing asymmetric resonators along the waveguide. By doing so, at a given frequency, three different wavevectors are excited, two of which with positive group velocity (T and F_{ip}), and one with negative group velocity (F_{op}). The physics involved gives rise to an energy flux competition between the different wave modes, redirecting energy with different polarisation and wave speed. However, as usually noticed in locking-based wave systems, the sudden change of the wavenumber induced by the periodic structure provides strong reflection. This mechanism, which is a physical consequence of the conservation of the crystal momentum, can be overcome by using graded structures [41,42], i.e by adiabatically modifying the wavenumber transformation along space. For this reason, in the last section a combination of roton-based and rainbow physics [43] is employed. This is achieved by gradually modify the geometry of the cell, and consequentially the dispersion curve, so that the relative maximum of the dispersion becomes the minimum in a subsequent cell. This implies that the frequency at which we can define the maximum of the dispersion curve, given by the interaction between torsion and flexural wave, will be the same frequency at which, later on in the structure, we will define, by engineering the change in geometry of the system, the relative minimum of the dispersion curve when the two flexural modes interact. This type of dispersion engineering shows that the wave is heavily localised in time and space in the metamaterial, (meaning that the energy of a travelling wave is confined in time and space for an extended time period) while also being efficiently converted into all the possible available modes that make up the roton-like dispersion. The result is a graded roton-like structure that is able to slow down a torsional incoming wave, convert it multiple times and finally give back a propagating in-plane flexural mode. The numerical and experimental results presented herein demonstrate how a simple structure can be used to confine and mode convert elastic waves, expanding the range of possibilities in the context of wave manipulation and control, with implications of technological relevance for applications involving mechanical vibrations, such as nondestructive evaluation, ultrasonic imaging, and energy harvesting. Moreover, the simultaneous coupling between waves with opposite energy fluxes paves the way for the development of effective delay-lines which can be used for sensing or signal amplification.

## 2. Designing the dispersion through mode locking

As stated above, the design implemented that grants the roton-like dispersion is obtained through the coupling between counter-propagating modes that results in the required maximum and minimum of the dispersion curve. This is possible thanks to the locking coupling mechanism that enables the interaction between two counter propagating modes that initially suffer accidental degeneracy [39,41]. By modifying the waveguide structure, it is possible to lift the degeneracy, create a small band-gap, and enable the interaction and the transfer of energy between the two modes in the vicinity of the band gap. If this mechanism is engineered twice on the same dispersion curve and by correctly stacking the modes in the right order and at the right frequency, the ending result is the roton-like dispersion relation. To obtain this result, the local group velocity of the three modes has to be engineered so that one of the three modes has a negative group velocity in the degeneracy region. After the coupling, the dispersion will have
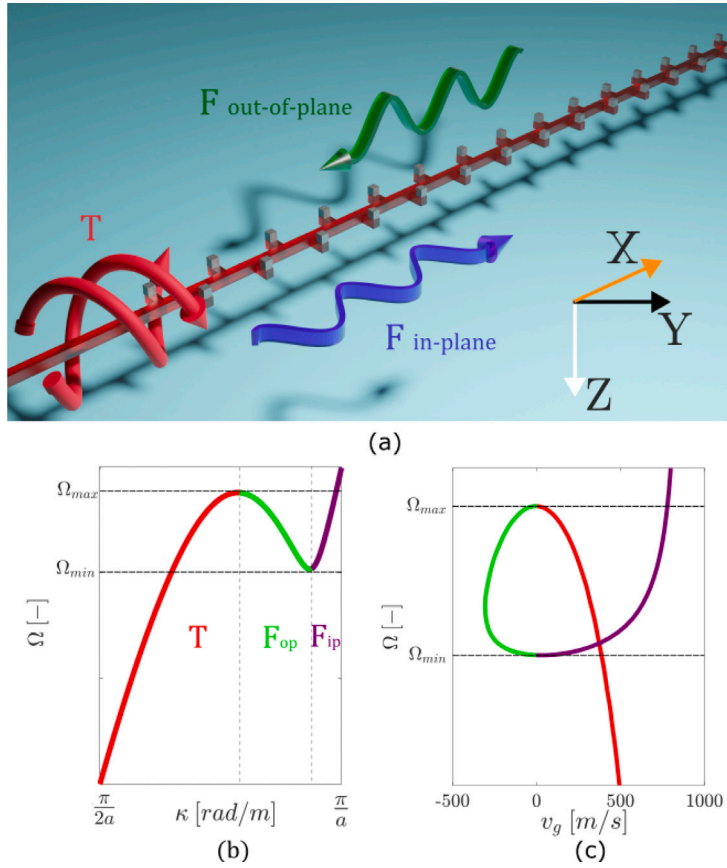
Fig. 1. (a) Rendering of the roton-like structure and the waves it supports and couples. The torsional wave, denoted with T (red spiral arrows), enters the metamaterial and it is initially mode converted into a counterpropagating out-of-plane flexural wave (F_{op}). In a second step, the out-of-plane flexural wave, with negative group velocity, couples while traversing the array with an in-plane flexural wave (F_{ip}). The wave coupling is obtained thanks to the brake in symmetry of the resonators along the wave propagation direction. Leveraging on this phenomenon, a dispersion relation with a local maximum and minimum within the First Brillouin Zone (FBZ) can be obtained. Such dispersion, named as roton-like, is depicted in (b), were each type of wave is colour coated. By inspecting the dispersion curve we notice the opposite group velocity of the out-of-plane flexural wave with respect to the torsional wave and the in-plane flexural wave, suggesting, at given frequency, competing energy fluxes. (c) Reports the group velocities proper of roton-like dispersion: positive, negative and zero group velocities. (For interpretation of the references to colour in this figure legend, the reader is referred to the web version of this article.)
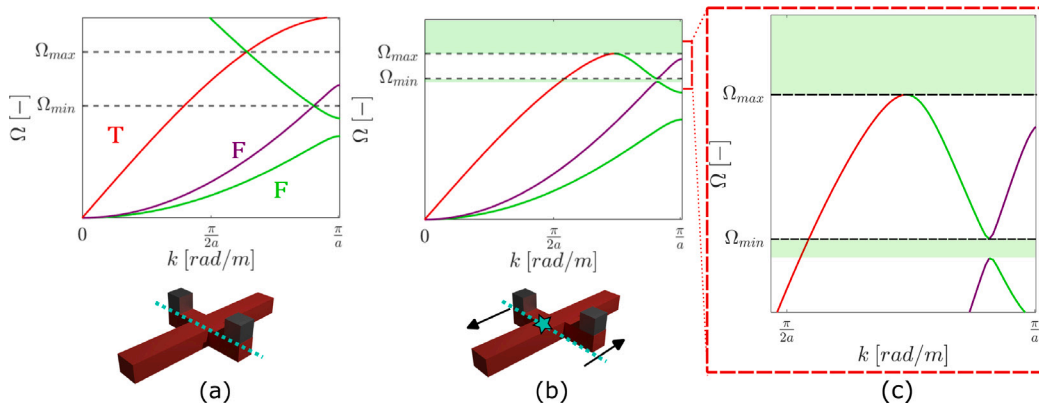
Fig. 2. Dispersion relation for the symmetric (degenerate) (a) and the shifted (lifted degeneracy) (b) cell. When the cell features (resonators) are mirror symmetric with respect to the plane perpendicular to the wave propagation direction (a), band crossings occurs between T, F_{op} and F_{ip} (marked with red, green and violet respectively). In such case, the eigenmodes are orthogonal, i.e. completely decoupled. By breaking the mirror symmetry the degeneracy is lifted, resulting in the creation of band-gaps and mode coupling. Leveraging on this phenomenon, a roton-like dispersion relation can be obtained, showing positive, negative and zero group velocities. This is the case depicted in the third branch of the dispersion in (b). (c) Reports an enlargement of (b). (For interpretation of the references to colour in this figure legend, the reader is referred to the web version of this article.)
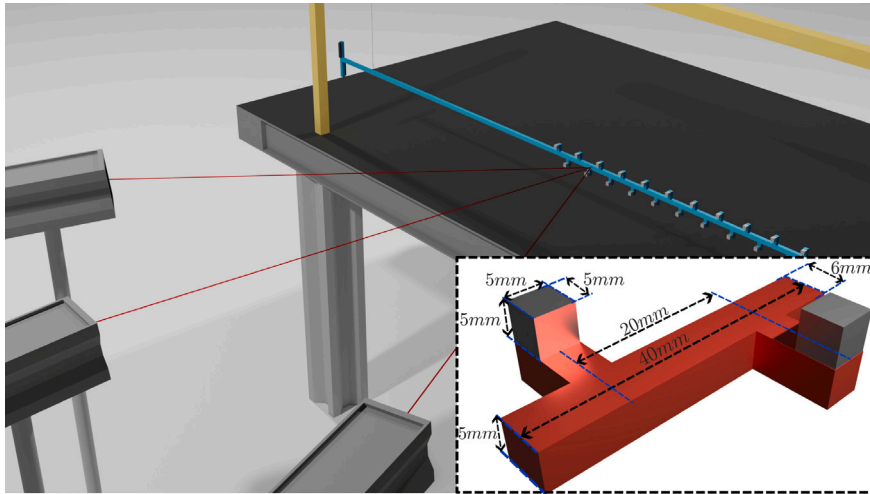
Fig. 3. Rendering of the experimental setup: the roton structure is hanged with wires, the input is given by a couple of resonators at the left end of the beam which are actuated out-of-phase using piezoelectric patches. Three heads of the Scanning Laser Doppler Vibrometer evaluate the velocity field inside the structure. On the bottom right the enlargement of the elementary cell's geometry that composes the periodic roton-like structure is reported.

two points of zero-group velocity (one that is a local maximum and one that is a local minimum) as it is shown in Fig. 1(b). To engineer the waveguide properties, it is first necessary to find and analyse a unit cell that is then periodically repeated to create an infinite waveguide; this is amenable to Floquet–Bloch theory and one extracts dispersion relations that relate the frequency to the Bloch wavenumber; the geometry we start with, Fig. 2 (a), has points of accidental degeneracy between three distinct branches of the dispersion relation. These points are necessary for the creation of band-gaps generated by lifting the degeneracy through the coupling of the wave modes. Fig. 2(b) reports the unit cell and the dispersion curves when the degeneracy is lifted. The twofold and simultaneous lift in degeneracy is given by a relative shift in position of the lateral resonators that, from a symmetric positioning in the cell in the degenerate case, get staggered. The final cell, the one used from this moment onward, is obtained by maximising the shift in relative position of the resonators that end up giving the cell a glide symmetry, that grants an elimination of the Bragg band gap. Moreover, Fig. 1(c) also reports the change of group velocity ($v_g = \frac{\partial \omega}{\partial k}$) of the roton-like dispersion branch with respect to frequency, colour coated depending on the relative mode considered. The phase velocity ($v_{ph} = \frac{\omega}{k}$) is always greater then 0, while the group velocity can be positive, zero and even negative in certain frequency ranges. The dispersion curves obtained up to now are all computed numerically by means of a Finite Element Model (FEM) using COMSOL Multiphysics® and imposing Bloch-Floquet boundary conditions on the elementary cell that makes up the metamaterial beam.

We validate numerically and experimentally the roton-like dispersion by inspecting, in time domain, the wave propagation along the periodic waveguide. The system is composed of twelve periodic cells so that a clear indication over the values of the wavevector in the periodic array can be obtained. A detailed description of the periodic structure and the experimental setup is shown in Fig. 3. The structure is made primarily of a steel beam ($E = 210$ GPa, $\rho = 7800$ Kg/m^3, $\nu = 0.23$), obtained from a plate using water jet cutting technology. The thickness is 5 mm while its width is 6 mm. The resonators, each 10 mm long and 5 mm wide, are positioned at a distance of 20 mm. We implement a tip mass to achieve the couplings needed (i.e. the interactions between the in-plane and out-of-plane modes). To simplify the fabrication process neodymium-iron-boron magnets of size $5 \times 5 \times 5$ mm (E = 150 GPa, $\rho = 8000$ Kg/m^3, $\nu = 0.3$) are used. The magnetic field is used to easily attach the tip masses, while its force does not interfere with the dynamic response of the system. The magnets are too far apart to interact between themselves and the magnetic field lines are deviated into the underlying steel structure. For this reason, in the numerical computation, the magnetic forces are neglected and the magnets are modelled as perfectly attached to the resonators' tips. The advantage of this structure is that it is very easy to manufacture with respect to current literature solutions [27,28], because it does not involve the use of complex three dimensional structures to couple far away cells, or magnetic systems.

For the experimental setup, we suspend the beam on a frame structure by means of elastic cables that do not affect the dynamics of the system [44,45]. The excitation signal is provided through a $KEYSIGHT$ 33500B waveform generator which synchronously starts with the measurement system. A narrowband source signal $V(t) = V_0 w(n) \sin(2\pi f_c)$ is used with amplitude $V_0 = 80$ V, Hann window $w(n)$, central frequency $f_c = 6000$ Hz and time duration 0.5 ms. The input is applied in the form of a torsional wave excitation; this is obtained experimentally by placing on one side of the waveguide a couple of resonators which are actuated out-of-phase using piezoelectric patches. The velocity field of the structure is measured using a Polytec 3D Scanning Laser Doppler Vibrometer (SLDV), that is able to measure and separate the 3D velocity field on the waveguide inside the array of resonators. To corroborate the roton-like dispersion of the structure, the time-domain wavefield is inspected when a narrowband input torsional wave is applied. Then the dispersion is evaluated by applying a two-dimensional (2D) Fast Fourier Transform (FFT) both in time and in space. It can be noticed that the numerical (Fig. 4(a)) and experimental (Fig. 4) (b) two-dimensional FFT of the wavefield are in good agreement with the expected roton-like dispersion. Specifically, we notice the peculiar maximum and minimum within the FBZ, together with positive and negative group velocity regions in the wavenumber space.
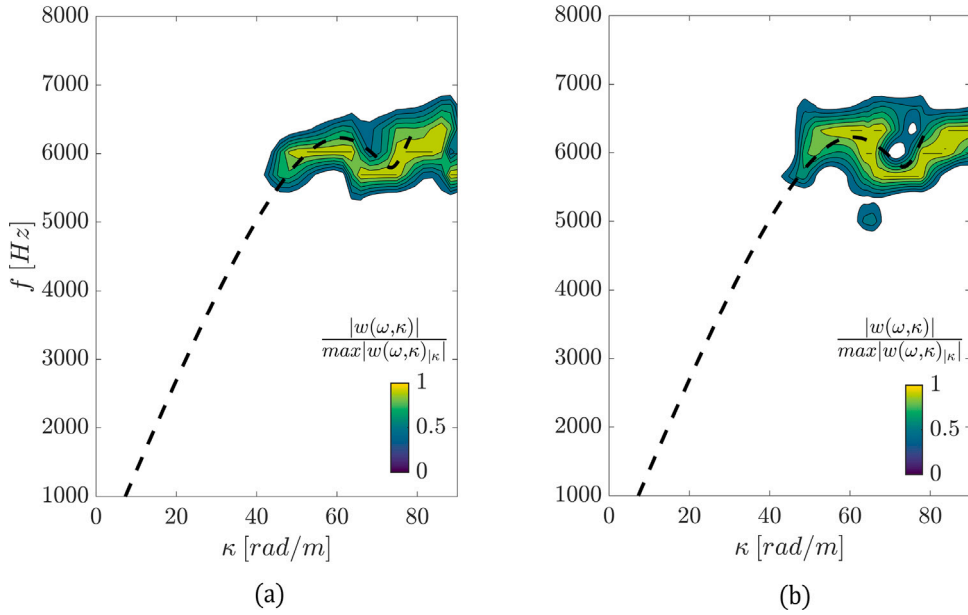
Fig. 4. Numerical and experimental dispersion relation of the roton-like structure. (a) Numerical result obtained from time domain analysis and (b) experimental results using the same input over the constructed geometry. The dashed black line is the numerical dispersion relation obtained through Bloch-Floquet boundary condition applied to the cell.

3. Adiabatic roton-like delay lines

Having obtained the roton-like dispersion is not effective for wave control given that the actual coupling between the modes does not allow one mode (the input wave) to efficiently and effectively follow all the positive and negative parts of the dispersion branch. In other words, a torsional wave sent to the structure would be mostly backscattered when the frequency is near the local maximum defined by the cell dispersion relation. This is a consequence of the conservation of crystal momentum, which induces reflections for fast and abrupt wavenumber transformations. To be more explicit, there is a sudden change of equivalent properties for a travelling wave between the plane beam and the roton periodic cell. The sudden change in wavevector implies, as for any wave impinging a different media, a strong reflected wave. For this reason, we opt for designing a graded roton-like structure. The aim is to implement an almost adiabatic grading (i.e. considering a slow variation of the fundamental Bloch mode of each cell along space [46,47]) of the system in the wavenumber space [41,42] so that the wave can be more efficiently converted into all the three modes. This mechanism, which enables a smooth change in the wavevector and consequently in the homogenised properties, facilitates the integration of the wave into the array, particularly because the mismatch in wavenumbers between the plain beam waveguide and the array is significantly reduced. To engineer the graded structure, the smooth change in properties is obtained by changing the distance between the resonators, and so the unit cells dimensions. Specifically, the geometry and the material properties of the cells remain the same (resonators lengths, width, tip mass), but the actual length of the cell is modified by changing the distance between the resonators. In the array, that is made of 25 cells, the cells are progressively enlarged starting from a length of 39 mm and ending the system with a length of 42 mm. This modifies the resulting roton-like dispersion as shown in Fig. 5. Here, the geometrical dimensions of the first and last unit cells of the graded structure are reported (Fig. 5(a)), together with a three-dimensional dispersion (Fig. 5(b)). It shows how the dispersion changes respectively with the enlargement of the cell. A level line is also present at the central frequency at which the analyses is performed. This is done to highlight the path that the wave is going to follow both in the real space and in the reciprocal space. The input is a torsionally polarised propagating wave, that enters the array. Then, inside the array (path (I)), the wave is slowed down and mode converted into a back propagating out-of-plane flexural mode. This happens progressively and it is over before it reaches the last cells of the adiabatic array. When converted, the back propagating out-of-plane flexural mode retraces the entire array (path (II)) and it is progressively converted into a propagating in-plane flexural mode near the beginning of the array. This new mode then propagates (path (III)) in the same direction as the first torsional wave from which it was generated. This final mode traverses again the entire array, finally exiting on the other side of the graded roton-like structure.

This hypothesis of enhancement of multiple wave conversion, coupled with the idea of creating an efficient delay line that converts a propagating torsion into a propagating flexural wave is studied both numerically and experimentally. From the numerical side, an implicit time-domain analysis is performed over the graded and periodic roton-like structures. Fig. 6 shows the results in the form of waterfall plots and spatiotemporal FFTs both in time and space. The arrays are both excited with the same input wave: a torsional wave centered at 6050 Hz. Both arrays are connected before and after to plain beams with the same dimension and
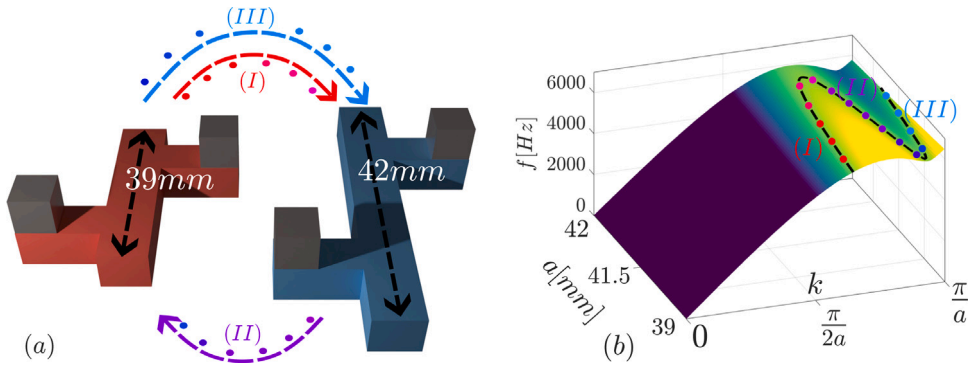
Fig. 5. (a) Geometry of the last and first cell of the graded roton-like array. The grading is obtained by varying the cell length, from 39 mm to 42 mm, keeping the resonators distanced half the cell length. (b) 3D representation of the dispersion relation in exam with respect to the normalised wavevector, the cell dimension and the frequency. The black dashed line is the path the wave follows during its propagation in the graded array. (I), (II), (III) Denote the paths that the different waves, with different group velocities, take while traversing the system and being slowed down and mode converted in the array. In (a) the paths are represented by the coloured dashed lines and the arrows show from which cell the waves start and arrive at. (c) Image of one of the specimens used for the experiments. (For interpretation of the references to colour in this figure legend, the reader is referred to the web version of this article.)

properties of the main beam that composes the backbone of the roton-like arrays. At both ends of these beams, Absorbing Layers using Increasing Damping (ALID) [48] are applied to avoid reflections that are generated either by the input wave or by the output modes of the array.

The numerical waterfall plots are reported in Fig. 6 for the graded (a,b) and periodic (d,e) structures. The wavefield along y and z directions is showed, where x is chosen parallel to the main beam axis, to be able to catch both the in-plane and out-of-plane flexural modes. More specifically y direction refers to the in plane direction and z to the out of plane (see Fig. 1). Moreover, to identify both torsional and flexural contributions, we opt for a line of points located on the edge of the waveguide; this choice is motivated by the negligible contribution of torsional waves on the displacement field along the central beam axis. In other words a torsional wave motion cannot be perceived if the analysis measures the displacement of points located on the beam axis, given that those points do not move. For this reason we analyse only a line of points the closest to the edge of the beam. Starting with the analysis of the graded roton array, we see that, for the in-plane motion (Fig. 6(a)), the input torsion is heavily scattered by the array. The wave that enters the array is deeply confined inside it in both time and space. The outputs given by the array are then twofold: there is a small component of torsional wave that exits the array (it is not converted by the adiabatic roton, but its intensity is very small), while a second component (and the most relevant one) is an in-plane flexural wave that, after a significant delay, exits the array. The in-plane flexural wave is the main wave we expect to see coming out of the array. That is because we applied two wave conversion mechanisms thanks to the graded or adiabatic locking effect in space. The distinction between the different modes is possible thanks to the very different group velocity of each mode. Moving to the analysis of the out-of-plane motion (Fig. 6(b)) we again see that the torsion enters the array, the wave is confined in the array and then it is backscattered after some time as an out-of plane flexural mode into the first waveguide. This continuous radiation of the wave signal is a typical behaviour of rainbow structures, denoted in acoustics as time spreading of the reflected pulse [49]. The structure is able to confine and radiate energy at specific time intervals, providing an effective wave conversion. The existence of propagating and reflected torsional waves is attributed to the grading, which is not gentle enough [41]. For this reason, the second conversion (out-of plane to in-plane) is not 100% efficient. Better results are to be expected (higher conversion efficiency) if the graded structure includes more cells. Fig. 6(c) shows the same results of 6 (a,b) but in the reciprocal space instead of the real space. To correctly detect the propagating F_{ip} and reflected F_{op}, we decide to focus on the positive wavenumber from the y displacement and the negative wavenumber from the z displacement. A strong amount of torsional wave is converted into flexural waves both in-plane and out-of-plane. To conclude the discussion over the results of the graded array, it can be said that the system acts according to the prediction of a double rainbow trapping effect [41]: given the two points of zero group velocity in the reciprocal space and the graded effect. The wave conversion is efficient and both flexural waves that are generated are first confined in the system and then exit the array after a significant time delay.

Now the results for the periodic roton-like array are analysed. For what concerns the in-plane solution (Fig. 6(d)) the input torsion is mostly backscattered or it traverses the system somewhat delayed. Moreover, a small flexural component can be seen after the array but it is very limited in intensity. A similar behaviour can be noticed for the out-of-plane solution (Fig. 6(e)), where most of the torsion is reflected and a small amount of the wave is converted. Finally, it can be seen that the wave is not localised in time and space (in the array) contrary to the graded case. This can be observed by examining the waterfall plot in the roton array region: in the adiabatic case, the displacement in both the y and z directions persists for a significantly longer duration compared to the non-adiabatic structure. Moving to the reciprocal space (Fig. 6(f)), the periodic structure is able to transfer a lower amount of energy onto the flexural modes with respect to the graded system. In conclusion, without the graded array, the propagating in-plane flexural mode cannot be efficiently generated, and that the wave is not strongly delayed.
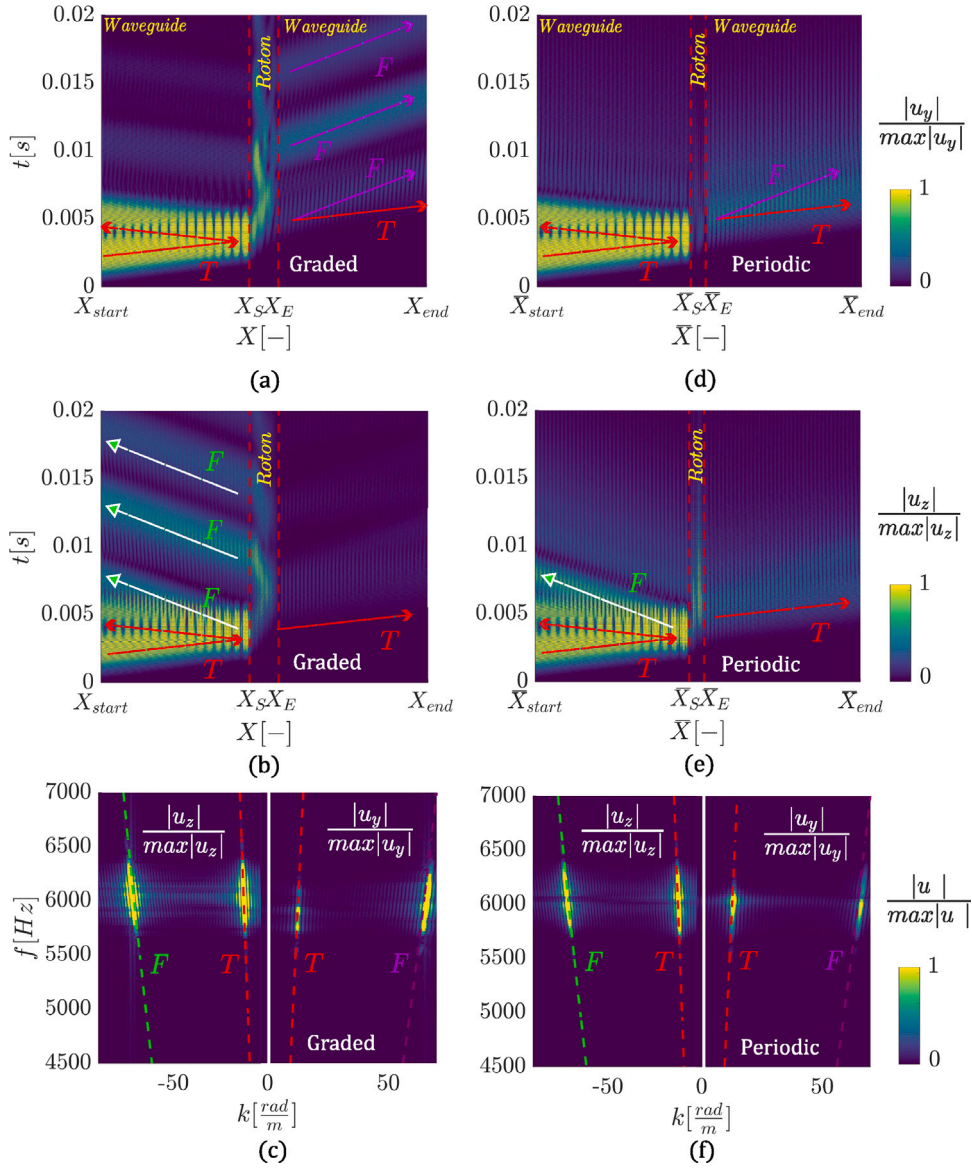
Fig. 6. Waterfall plots and spatiotemporal FFTs from time domain analyses over both the graded (a, b, c) and the periodic (d, e, f) structures. The structures are connected to an elastic waveguide on both sides, with absorbing boundary conditions. Results are obtained by taking a line of points on one edge of the waveguide to show both the input and output waves. The displacement along y-direction is inspected to catch the in-plane behaviour (F_{ip}), while the displacement along z-direction is measured to describe the out-of plane response (F_{op}). By comparing the waterfall plots (a,d) - (b,e), a stronger conversion of flexural waves is observed in the graded structure. Similarly, the FFT from the graded structure (c) shows a stronger wavenumber contribution of both F_{op} and F_{ip} with respect to the periodic case (f).

The same structures are tested experimentally using the setup reported in Fig. 3. The only difference with respect to the numerical simulations is the length of the waveguide before and after the array, which is not infinite (for obvious reasons). This limitation has two implications: (i) the input signal, generated by the piezoelectric patches, has to be shorter to properly see a propagating wave and so the excited frequencies are more spread out; (ii) since we want to scan the entire length of the structure, a lower resolution along the beam width is expected. For this reason, the points are taken on the central line axis of the beam, resulting in a less clear indication of the input torsional wave. The input is provided by two out-of-phase piezoelectric patches positioned over two lateral resonators at the beginning of the waveguide (same configuration of Fig. 3). The results are reported in Fig. 7 in the form of waterfall plots and FFTs. We can clearly distinguish the difference between the graded roton-like array and the periodic one. Even though the results are not as clear as the numerical ones, mainly because of the absence of absorbing boundary conditions and the presence of imperfections in the specimen, the overall behaviour expected is maintained. The graded structure better converts the
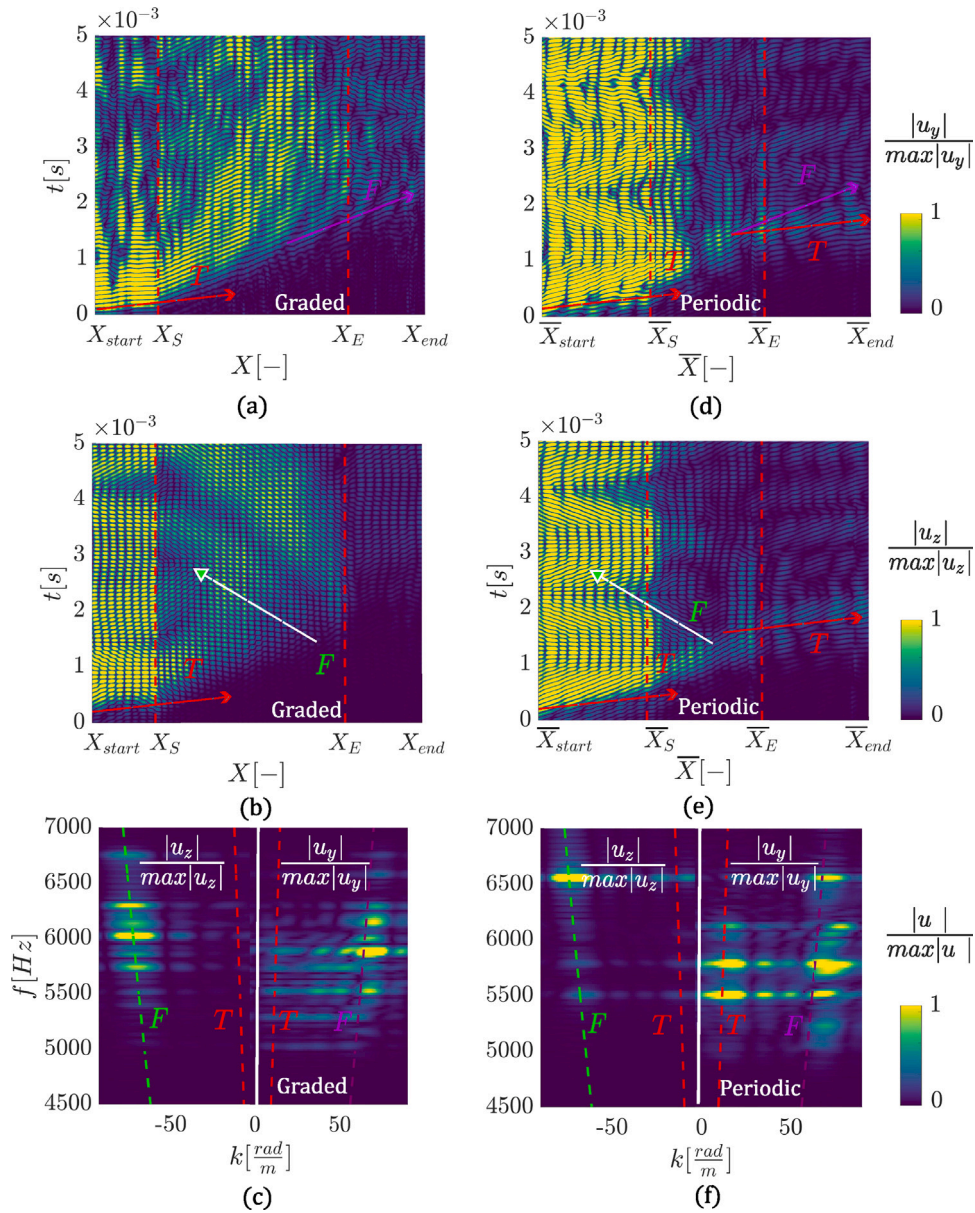
Fig. 7. Experimental waterfall plots and spatiotemporal FFTs over both the graded (a, b, c) and the periodic (d, e, f) structures. Differently with respect to the numerical results, both structures are of finite lengths, thus allowing for spurious reflections. Results are obtained by taking a line of points on the waveguide axis; for this reason, torsional waves are not fully detected. As for the numerical results, a stronger conversion of flexural waves is observed for the adiabatic structure. This is particularly visible from the FFTs, where we notice a higher contribution of F_{ip} and F_{op} in the graded structure (c) with respect to the periodic one (f).

input torsion into the two flexural modes, while the periodic array is less able to do so and we see a major contribution given by the torsional mode, both in the FFT space and the waterfall plots.

4. Conclusions and perspectives

A roton-like dispersion relation for an elastic waveguide was engineered and studied both numerically and experimentally. The change in wave polarisation is the key ingredient to obtain such unusual dispersion without implementing connections between non-nearest neighbours. The creation of a local maximum and minimum is given by the coupling through wave locking of different wave modes that, thanks to the staggered resonators, interact and exchange energy. The resulting effect is that waves with different wavelengths and group velocity propagate simultaneously in opposite directions inside the array. The roton-like nature of the

dispersion relation has been validated both numerically and experimentally. Furthermore, we also demonstrated how to enhance the energy exchange between the modes in the roton-like array by spatially modifying the parameters of the elementary cell, i.e. leveraging the rainbow effect. By introducing a grading, a double rainbow trapping effect was created, allowing for a wave confinement in the array for extended periods of time. The focus though was mainly on studying the resulting waves that are radiated from the array after extended time intervals. The most interesting one is the in-plane flexural wave that is generated after a strong delay and is then mostly the only wave that is outputted on the other side of the rainbow array. The experiments also showed the importance of the graded array, and reproduced, with some differences given by the complications of having finite structures, the results shown numerically. In the end, the graded roton-like waveguide we propose has the features of not having complicated fabrication methods to obtain the dispersion requested and it can be easily tuned to the needed frequencies. The results show promising avenues both for structures that implement mode coupling as a tool for dispersion engineering and the synergy that these systems have with graded arrays. Signal control can be achieved to create delay lines and elastic energy localisation zones, useful tools for energy harvesting applications.

CRediT authorship contribution statement

L. Iorio: Conceptualization, Writing – original draft, Review, Methodology, Investigation, Visualization. **J.M. De Ponti:** Writing – original draft, Review, Methodology, Investigation, Validation. **F. Maspero:** Writing – original draft. **R. Ardito:** Writing – original draft, Review, Supervision, Project administration, Funding acquisition.

Declaration of competing interest

The authors declare that they have no known competing financial interests or personal relationships that could have appeared to influence the work reported in this paper.

Data availability

Data will be made available on request.

Acknowledgements

References

[1] F. Lemoult, M. Fink, G. Lerosey, Acoustic resonators for far-field control of sound on a subwavelength scale, Phys. Rev. Lett. 107 (2011) 064301, http://dx.doi.org/10.1103/PhysRevLett.107.064301, URL https://link.aps.org/doi/10.1103/PhysRevLett.107.064301.

[2] V. Laude, Phononic Crystals Artificial Crystals for Sonic, Acoustic, and Elastic Waves, Vol. 26, De Gruyter Studies in Mathematical Physics, 2015, http://dx.doi.org/10.1515/9783110641189, URL https://www.degruyter.com/document/doi/10.1515/9783110641189/html.

[3] R. Ardito, M. Cremonesi, L. D'Alessandro, A. Frangi, Application of optimally-shaped phononic crystals to reduce anchor losses of MEMS resonators, 2016-November, 2016, http://dx.doi.org/10.1109/ULTSYM.2016.7728780, URL https://ieeexplore.ieee.org/document/7728780,

[4] Y. Achaoui, T. Antonakakis, S. Brûlé, R.V. Craster, S. Enoch, S. Guenneau, Clamped seismic metamaterials: Ultra-low frequency stop bands, New J. Phys. 19 (2017) http://dx.doi.org/10.1088/1367-2630/aa6e21, URL https://iopscience.iop.org/article/10.1088/1367-2630/aa6e21/meta.

[5] A. Krushynska, M. Miniaci, F. Bosia, N. Pugno, Coupling local resonance with bragg band gaps in single-phase mechanical metamaterials, Extreme Mech. Lett. 12 (2017) 30–36, http://dx.doi.org/10.1016/j.eml.2016.10.004, URL https://www.sciencedirect.com/science/article/pii/S2352431616300542, Frontiers in Mechanical Metamaterials.

[6] L. D'Alessandro, A. Krushynska, R. Ardito, N. Pugno, A. Corigliano, A design strategy to match the band gap of periodic and aperiodic metamaterials, Sci. Rep. 10 (1) (2020) http://dx.doi.org/10.1038/s41598-020-73299-3, URL https://www.nature.com/articles/s41598-020-73299-3.

[7] M. Moscatelli, R. Ardito, L. Driemeier, C. Comi, Band-gap structure in two-and three-dimensional cellular locally resonant materials, J. Sound Vib. 454 (2019) 73–84, http://dx.doi.org/10.1016/j.jsv.2019.04.027, URL https://www.sciencedirect.com/science/article/pii/S0022460X1930238X.

[8] G. Aguzzi, C. Kanellopoulos, R. Wiltshaw, R.V. Craster, E.N. Chatzi, A. Colombi, Octet lattice-based plate for elastic wave control, Sci. Rep. 12 (1088) (2022) 1–14, http://dx.doi.org/10.1038/s41598-022-04900-0, URL https://www.nature.com/articles/s41598-022-04900-0.

[9] J.M. De Ponti, A. Colombi, E. Riva, R. Ardito, F. Braghin, A. Corigliano, R.V. Craster, Experimental investigation of amplification, via a mechanical delay-line, in a rainbow-based metamaterial for energy harvesting, Appl. Phys. Lett. 117 (143902) (2020) 1–6, http://dx.doi.org/10.1063/5.0023544, URL https://aip.scitation.org/doi/10.1063/5.0023544.

[10] B. Zhao, H.R. Thomsen, J.M. De Ponti, E. Riva, B. Van Damme, A. Bergamini, E. Chatzi, A. Colombi, A graded metamaterial for broadband and high-capability piezoelectric energy harvesting, Energy Convers. Manag. 269 (2022) 116056, http://dx.doi.org/10.1016/j.enconman.2022.116056, URL https://www.sciencedirect.com/science/article/pii/S0196890422008445.

[11] J.M. De Ponti, E. Riva, F. Braghin, R. Ardito, Elastic three-dimensional metaframe for selective wave filtering and polarization control, Appl. Phys. Lett. 119 (21) (2021) 211903, http://dx.doi.org/10.1063/5.0065553, URL https://aip.scitation.org/doi/10.1063/5.0065553.

[12] G.J. Chaplain, J.M. De Ponti, The elastic spiral phase pipe, J. Sound Vib. 523 (2022) 116718, http://dx.doi.org/10.1016/j.jsv.2021.116718, URL https://www.sciencedirect.com/science/article/pii/S0022460X21007185.

[13] M.P. Makwana, R.V. Craster, Geometrically navigating topological plate modes around gentle and sharp bends, Phys. Rev. B 8 (2018) 1–12.

[14] J. Cha, K.W. Kim, C. Daraio, Experimental realization of on-chip topological nanoelectromechanical metamaterials, 564, 2018, pp. 229–233, http://dx.doi.org/10.1038/s41586-018-0764-0, URL https://www.nature.com/articles/s41586-018-0764-0.

[15] Y. Xia, A. Erturk, M. Ruzzene, Topological edge states in quasiperiodic locally resonant metastructures, Phys. Rev. A 13 (2020) 014023, http://dx.doi.org/10.1103/PhysRevApplied.13.014023, URL https://link.aps.org/doi/10.1103/PhysRevApplied.13.014023.

[16] H. Chen, H. Nassar, G. Huang, A study of topological effects in 1D and 2D mechanical lattices, J. Mech. Phys. Solids 117 (2018) 22–36, http://dx.doi.org/10.1016/j.jmps.2018.04.013, URL https://www.sciencedirect.com/science/article/pii/S0022509618301820.

[17] H. Nassar, B. Yousefzadeh, R. Fleury, M. Ruzzene, A. Alù, C. Daraio, A.N. Norris, G. Huang, H.M. R., Nonreciprocity in acoustic and elastic materials, Nat. Rev. Mat. 5 (2020) 667–685, http://dx.doi.org/10.1038/s41578-020-0206-0, URL https://www.nature.com/articles/s41578-020-0206-0#citeas.

[18] G. Chaplain, J.M. De Ponti, G. Aguzzi, A. Colombi, R.V. Craster, Topological rainbow trapping for elastic energy harvesting in graded Su-Schrieffer-Heeger systems, Phys. Rev. A 14 (2020) 054035, http://dx.doi.org/10.1103/PhysRevApplied.14.054035, URL https://link.aps.org/doi/10.1103/PhysRevApplied.14.054035.

[19] P. Wang, L. Lu, K. Bertoldi, Topological phononic crystals with one-way elastic edge waves, Phys. Rev. Lett. 115 (2015) 104302, http://dx.doi.org/10.1103/PhysRevLett.115.104302, URL https://link.aps.org/doi/10.1103/PhysRevLett.115.104302.

[20] A. Souslov, B.C. Van Zuiden, D. Bartolo, V. Vitelli, Topological sound in active-liquid metamaterials, Nat. Phys. 13 (2017) 1091–1094, http://dx.doi.org/10.1038/nphys4193, URL https://www.nature.com/articles/nphys4193#citeas.

[21] S. Shankar, A. Souslov, M.J. Bowick, M.C. Marchetti, V. Vitelli, Topological active matter, Nat. Rev. Phys. 4 (2022) 380–398, http://dx.doi.org/10.1038/s42254-022-00445-3, URL https://www.nature.com/articles/s42254-022-00445-3#citeas.

[22] S.H. Mousavi, A.B. Khanikaev, Z. Wang, Topologically protected elastic waves in phononic metamaterials, Nature Commun. 6 (2015) 1–5, http://dx.doi.org/10.1038/ncomms9682, URL https://www.nature.com/articles/ncomms9682#citeas.

[23] J.M. De Ponti, L. Iorio, G.J. Chaplain, A. Corigliano, R.V. Craster, R. Ardito, Tailored topological edge waves via chiral hierarchical metamaterials, Phys. Rev. A 19 (2023) 034079, http://dx.doi.org/10.1103/PhysRevApplied.19.034079, URL https://link.aps.org/doi/10.1103/PhysRevApplied.19.034079.

[24] J.M. De Ponti, L. Iorio, E. Riva, F. Braghin, A. Corigliano, R. Ardito, Enhanced energy harvesting of flexural waves in elastic beams by bending mode of graded resonators, Front. Mater. 8 (2021) 1–7, http://dx.doi.org/10.3389/fmats.2021.745141, URL https://www.frontiersin.org/articles/10.3389/fmats.2021.745141/full.

[25] A. Colombi, D. Colquitt, P. Roux, S. Guenneau, R.V. Craster, A seismic metamaterial: The resonant metawedge, Sci. Rep. 6 (2016) 27717, http://dx.doi.org/10.1038/srep27717, URL https://www.nature.com/articles/srep27717.

[26] G.J. Chaplain, J.M. De Ponti, A. Colombi, R. Fuentes-Dominguez, P. Dryburg, D. Pieris, R.J. Smith, A. Clare, M. Clark, R.V. Craster, Tailored elastic surface to body wave umklapp conversion, Nature Commun. 11 (3267) (2020) http://dx.doi.org/10.1038/s41467-020-17021-x, URL https://www.nature.com/articles/s41467-020-17021-x#citeas.

[27] Y. Chen, M. Kadic, M. Wegener, Roton-like acoustical dispersion relations in 3D metamaterials, Nature Commun. 12 (3278) (2021) 1–8, http://dx.doi.org/10.1038/s41467-021-23574-2, arXiv:https://www.science.org/doi/pdf/10.1126/sciadv.abm2189, URL https://www.nature.com/articles/s41467-021-23574-2.

[28] J.A.I. Martínez, M.F. Groß, Y. Chen, T. Frenzel, V. Laude, M. Kadic, M. Wegener, Experimental observation of roton-like dispersion relations in metamaterials, Sci. Adv. 7 (49) (2021) eabm2189, http://dx.doi.org/10.1126/sciadv.abm2189, arXiv:https://www.science.org/doi/pdf/10.1126/sciadv.abm2189, URL https://www.science.org/doi/abs/10.1126/sciadv.abm2189.

[29] L. Landau, Theory of the superfluidity of Helium II, Phys. Rev. 60 (1941) 356–358, http://dx.doi.org/10.1103/PhysRev.60.356, URL https://link.aps.org/doi/10.1103/PhysRev.60.356.

[30] R.P. Feynman, M. Cohen, Energy spectrum of the excitations in liquid helium, Phys. Rev. 102 (1956) 1189–1204, http://dx.doi.org/10.1103/PhysRev.102.1189, URL https://link.aps.org/doi/10.1103/PhysRev.102.1189.

[31] H.R. Glyde, A. Griffin, Zero sound and atomiclike excitations: The nature of phonons and rotons in liquid ^{4}He, Phys. Rev. Lett. 65 (1990) 1454–1457, http://dx.doi.org/10.1103/PhysRevLett.65.1454, URL https://link.aps.org/doi/10.1103/PhysRevLett.65.1454.

[32] H. Godfrin, K. Beauvois, A. Sultan, E. Krotscheck, J. Dawidowski, B. Fåk, J. Ollivier, Dispersion relation of Landau elementary excitations and thermodynamic properties of superfluid ^{4}He, Phys. Rev. B 103 (2021) 104516, http://dx.doi.org/10.1103/PhysRevB.103.104516, URL https://link.aps.org/doi/10.1103/PhysRevB.103.104516.

[33] J. Kishine, A.S. Ovchinnikov, A.A. Tereshchenko, Chirality-induced phonon dispersion in a noncentrosymmetric micropolar crystal, Phys. Rev. Lett. 125 (2020) 245302, http://dx.doi.org/10.1103/PhysRevLett.125.245302, URL https://link.aps.org/doi/10.1103/PhysRevLett.125.245302.

[34] L. Brillouin, Wave Propagation in Periodic Structures, Electric Filters and Crystal Lattices, McGraw-Hill Book Company, Inc., New York, 1946.

[35] A. Carcaterra, F. Coppo, F. Mezzani, S. Pensalfini, Long-range retarded elastic metamaterials: Wave-stopping, negative, and hypersonic or superluminal group velocity, Phys. Rev. A 11 (2019) 014041, http://dx.doi.org/10.1103/PhysRevApplied.11.014041, URL https://link.aps.org/doi/10.1103/PhysRevApplied.11.014041.

[36] A. Rezaei, F. Mezzani, A. Carcaterra, Wave propagation with long-range forces and mistuning effects, Proc. Inst. Mech. Eng. C. J. Mech. Eng. Sci. 235 (14) (2021) 2622–2628, http://dx.doi.org/10.1177/0954406221989743.

[37] W. Lacarbonara, B. Balachandran, J. Ma, J.A.T. Machado, G. Stepan, New Trends in Nonlinear Dynamics: Proceedings of the International Nonlinear Dynamics Conference NODYCON 2019, Springer Nature, 2020, pp. 1–380, URL https://link.springer.com/content/pdf/bfm:978-3-030-34724-6/1.pdf.

[38] A. Corigliano, R. Ardito, C. Comi, A. Frangi, A. Ghisi, Mechanics of Microsystems, John Wiley '&' Sons Inc, 2017, http://dx.doi.org/10.1002/9781119053828, URL https://onlinelibrary.wiley.com/doi/book/10.1002/9781119053828.

[39] B.R. Mace, E. Manconi, Wave motion and dispersion phenomena: Veering, locking and strong coupling effects, J. Acoust. Soc. Am. 131 (2012) http://dx.doi.org/10.1121/1.3672647, URL https://asa.scitation.org/doi/10.1121/1.3672647.

[40] G.J. Chaplain, D. Pajer, J.M. De Ponti, R.V. Craster, Delineating rainbow reflection and trapping with applications for energy harvesting, New J. Phys. 22 (063024) (2020) 1–13, http://dx.doi.org/10.1088/1367-2630/ab8cae, URL https://iopscience.iop.org/article/10.1088/1367-2630/ab8cae.

[41] J.M. De Ponti, L. Iorio, E. Riva, R. Ardito, F. Braghin, A. Corigliano, Selective mode conversion and rainbow trapping via graded elastic waveguides, Phys. Rev. A 16 (2021) 034028, http://dx.doi.org/10.1103/PhysRevApplied.16.034028, URL https://link.aps.org/doi/10.1103/PhysRevApplied.16.034028.

[42] J.M. De Ponti, L. Iorio, R. Ardito, Graded elastic meta-waveguides for rainbow reflection, trapping and mode conversion, EPJ Appl. Metamater. 9 (2022) 1–5, http://dx.doi.org/10.1051/epjam/2022004, URL https://epjam.epj.org/articles/epjam/abs/2022/01/epjam210018/epjam210018.html.

[43] K.L. Tsakmakidis, A.D. Boardman, O. Hess, 'Trapped rainbow' storage of light in metamaterials, Nature 450 (7168) (2007) 397–401, http://dx.doi.org/10.1038/nature06285.

[44] D. Rovšček, J. Slavič, M. Boltežar, The use of strain sensors in an experimental modal analysis of small and light structures with free–free boundary conditions, J. Vib. Control 19 (7) (2013) 1072–1079, http://dx.doi.org/10.1177/1077546312445058.

[45] D.T. Griffith, T.G. Carne, J.A. Paquette, Modal testing for validation of blade models, Wind Eng. 32 (2) (2008) 91–102, http://dx.doi.org/10.1260/030952408784815817.

[46] O. Schnitzer, Waves in slowly varying band-gap media, SIAM J. Appl. Math. 77 (4) (2017) 1516–1535, http://dx.doi.org/10.1137/16M110784X.

[47] S.G. Johnson, P. Bienstman, M.A. Skorobogatiy, M. Ibanescu, E. Lidorikis, J.D. Joannopoulos, Adiabatic theorem and continuous coupled-mode theory for efficient taper transitions in photonic crystals, Phys. Rev. E 66 (2002) 066608, http://dx.doi.org/10.1103/PhysRevE.66.066608, URL https://link.aps.org/doi/10.1103/PhysRevE.66.066608.

[48] P. Rajagopal, M. Drozdz, E.A. Skelton, M.J. Lowe, R.V. Craster, On the use of absorbing layers to simulate the propagation of elastic waves in unbounded isotropic media using commercially available finite element packages, NDT & E Int. 51 (2012) 30–40, http://dx.doi.org/10.1016/j.ndteint.2012.04.001, URL https://www.sciencedirect.com/science/article/pii/S0963869512000515.

[49] A. Cebrecos, R. Picó, V.J. Sánchez-Morcillo, K. Staliunas, V. Romero-García, L.M. Garcia-Raffi, Enhancement of sound by soft reflections in exponentially chirped crystals, AIP Adv. 4 (2014) 124402, http://dx.doi.org/10.1063/1.4902508.